INTERNATIONAL JOURNAL OF ROBUST AND NONLINEAR CONTROL
Int. J. Robust Nonlinear Control 2009; **19**:185–217
Published online 6 March 2008 in Wiley InterScience (www.interscience.wiley.com). DOI: 10.1002/rnc.1308

Comparison between a switching controller and two LTI controllers for a class of LTI plants

Keith R. Santarelli*, † and Munther A. Dahleh

Laboratory for Information and Decision Systems, Massachusetts Institute of Technology, 77 Massachusetts Avenue, Cambridge, MA 02139, U.S.A.

SUMMARY

We consider the design of three different control architectures for a step response tracking problem within a class of linear time-invariant (LTI) plants. Our goal is to motivate the use of a particular switching architecture that has been the subject of our prior work. We present the design of the particular switching architecture that we use and characterize its step response performance (measured in terms of the percentage overshoot and 1% settling time of the step response). We then compare the response of the switching controller with two other forms of LTI control in a servo configuration, one in which the order of the controller is constrained to be first order (which matches the order of the dynamics of the switching controller) and one in which the order of the controller is unconstrained. We will show that the switching architecture can outperform first-order LTI control, first in the context of a particular example. We shall then provide a weak generalization to extend this result to a more general class of plants. We shall also show that, while the LTI control of unconstrained order can outperform the switching architecture, the performance improvement is bounded (in a sense to be defined). Moreover, one method of designing close-to-optimal controllers will be discussed, which yields controllers of very high order. Copyright © 2008 John Wiley & Sons, Ltd.

Received 5 June 2007; Revised 30 September 2007; Accepted 8 January 2008

KEY WORDS: switching systems; hybrid systems; controller design; overshoot; settling time

1. INTRODUCTION

The study of switching systems has received a great deal of attention in the systems literature for over a decade (see, e.g. [1–6]). In particular, the problem of stabilizing a continuous-time system via hybrid output feedback has received a great amount of attention (see, e.g. [7–17]). Our previous

*Correspondence to: Keith R. Santarelli, Laboratory for Information and Decision Systems, Massachusetts Institute of Technology, 77 Massachusetts Avenue, Rm 32D-758, Cambridge, MA 02139, U.S.A.
†E-mail: krsanta@mit.edu

Contract/grant sponsor: Air Force Aerospace OSR; contract/grant number: FA9550-04-1-0052

work has focused on a particular subproblem within this larger domain and is specifically related to stabilizability of second-order linear systems via switched proportional gain feedback; Santarelli *et al.* [12] provide a set of necessary and sufficient conditions for which a given second-order plant is stabilizable via switched proportional gain feedback, and a specific switching control law is provided when stability is possible; Santarelli *et al.* [13] extend the first result by considering an optimal control problem in which the objective is to stabilize a second-order linear time-invariant (LTI) system via switched proportional gain feedback in a manner which maximizes the rate of convergence of the state trajectory to the origin.

The goal of this paper is to apply the control laws that are obtained in our previous results to a particular application, namely the design of switching controllers to asymptotically track step inputs for a class of second-order plants. The specific class we consider are those plants that take the form

$$P(s)=\frac{a}{s(s-b)} \tag{1}$$

where $a>0, b\in\mathbf{R}$, and $b^2\leqslant a$. While we defer a formal explanation of the condition $b^2\leqslant a$ until a later section, enforcement of this constraint can be viewed as examining a class of plants which are perturbations of a nominal plant $P(s)=1/s^2$. We shall assess the quality of the step response in terms of the percentage overshoot and 1% settling time when the input is a step, i.e. for an exogenous input $r(t)$ of the form

$$r(t)=\begin{cases}0, & t<0\\ r, & t\geqslant 0\end{cases}$$

with $r>0$. Under the assumption that the step response $s(t)$ asymptotically tracks the input $r(t)$, then for a step input of amplitude $r>0$, we define the percentage overshoot of the zero-state unit step response $s(t)$ as the smallest value of $M>0$ such that

$$s(t)\leqslant r(M+1) \quad \forall t>0$$

and define the 1% settling time as the smallest value of $T>0$ such that

$$|s(t)-r|\leqslant 0.01r \quad \forall t\geqslant T$$

Our objective in this exposition is as follows: we wish to compare the performance that can be achieved via the particular switching architecture that we shall examine (in terms of the above performance measures) with the performance that can be achieved via two different forms of LTI control. Our first comparison will investigate the step response performance on an LTI feedback controller connected in a *servo* configuration where the continuous-time LTI controller $K(s)$ is of first order (which matches the order of the dynamics of the switching controller). We shall first examine a case study for the case in which the plant is a double integrator ($P(s)=1/s^2$) and shall show that the switching architecture outperforms the first-order LTI controller in this case. We shall then provide a weak generalization that will allow us to conclude that similar performance benefits can be guaranteed for a more general class of second-order plants.

Our second comparison will investigate the step response performance of a rational LTI controller connected in a servo configuration where the order of the controller $K(s)$ is unconstrained. Such a comparison will allow us to obtain some information about the relative performance of our switching architecture to certain fundamental limits of LTI control in a particular feedback configuration.

DOI: 10.1002/rnc

One may naturally expect that the performance of an LTI controller of unconstrained order will outperform a first-order switching controller, and, indeed, this turns out to be the case here; however, as we will show, the performance gap between the switching architecture and what is achievable via LTI control is *bounded* (in a sense to be defined), and an algorithm for designing LTI controllers that yield close-to-optimal performance will be shown to produce controllers of rather high order.

During the preparation of this manuscript, it was pointed out that the result of Santarelli *et al.* [12] is similar to the results of [18] and [19], with the exception that the framework of [12] employs continuous-time nonlinear feedback laws, while [18] and [19] employ hybrid feedback automata. The reader who is interested in exploring the differences between the switched feedback approach we take here and the hybrid feedback approach of [18] and [19] is encouraged to explore these two references.

As a note, all of the material presented here is an expanded version of a conference paper [20]. All of the material present in [20] is present in this exposition and is reproduced with permission.

2. SWITCHING ARCHITECTURE DESIGN

A block diagram of the switching architecture to be designed in this section is depicted in Figure 1. Several comments are in order. First, the block labeled '± 1' switches between proportional gains of $+1$ and -1, i.e. $u(t)=e(t)$ or $u(t)=-e(t)$ for all times. It is the function of the two blocks on the upper level of the block diagram to create an appropriate switching signal $\sigma(t)$ such that the closed-loop dynamics are stable and the plant output $y(t)$ asymptotically tracks the input $r(t)$ when $r(t)$ is a step input. The block labeled '$v(\cdot,\cdot)$' is a memoryless switching law that takes the form

$$v(z)=\begin{cases}-1, & z'Mz\leqslant 0\\ 1, & z'Mz>0\end{cases} \tag{2}$$

where $z=[e\ \ \hat{x}_2]'$ and M is a symmetric matrix. In layman's terms, the switching law $v(z)$ chooses one value of gain inside a sector of the $e-\hat{x}_2$ plane and chooses another value of the gain in a complementary sector. The block labeled 'Observer' is a first-order LTI system whose function is to provide a partial state estimate of the plant $P(s)$.

The motivation for investigating the switching architecture of Figure 1 stems from a general interest in the design of switching systems in which the analog control input to the plant is

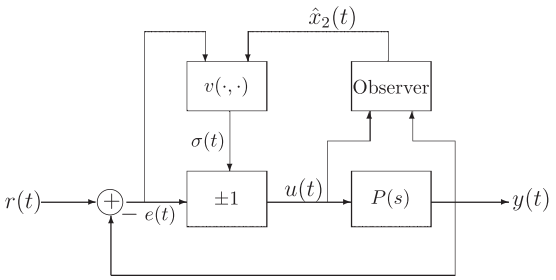

Figure 1. Proposed switching architecture to be used in designing a controller that asymptotically tracks a step input.

DOI: 10.1002/rnc

constrained to be simple in some sense. Such problems arise, for instance, in the electronics industry where the design of feedback compensators for operational amplifier circuits is typically not higher than first-order feedback compensators [21, 22]. We consider the problem of switching between proportional gains (the block labeled '± 1' in Figure 1) since this is simple from an implementation-level perspective and because the closed-loop dynamics of the overall feedback interconnection are often simple enough to analyze via elementary techniques, hence allowing us to make concrete mathematical statements while gaining some insight into the problem-at-large of switching under constrained control actions. It is not obvious that the switching architecture of Figure 1 will provide any performance benefits over a first-order linear controller due to the simplicity of the proportional gain analog control action, but, as we shall show in our first comparison, this is indeed the case.

The motivation for choosing switching gains of $+1$ and -1 as indicated in the block diagram of Figure 1 is due to a constraint that we shall impose on the design of the linear controller structures in subsequent sections. In order to make sure that the linear controllers that we design provide 'reasonable' control inputs, we shall impose the constraint that the control signal $u(t)$ be bounded for all times. Specifically, we shall impose the constraint that when $r(t)$ is a *unit* step input, the control signal $u(t)$ must satisfy $|u(t)| \leqslant 1$ for all $t \geqslant 0$.

To see how the above constraint affects the choice of switching gains, consider an implementation where we switch between gains of $+K$ and $-K$, $K>0$. As we will show now, the constraint that $|u(t)| \leqslant 1$ for all $t \geqslant 0$ implies that $0<K \leqslant 1$. Indeed, under the assumption of zero initial state, $|u(0)| = K|r(0)| = K$ when $r(t)$ is a unit step input, and it immediately follows that K must be less than or equal to 1. We shall show in a later section that the condition $0<K \leqslant 1$ does in fact guarantee that $|u(t)| \leqslant 1$ for *all* $t \geqslant 0$. We choose to study the specific case where $K=1$ since this value of K maximizes the rate of convergence of the state trajectories to the origin when the input $r(t)=0$ (see [12]). It may be unclear as to why we wish to choose the value of K in this way, but, as we shall see, the zero-state step response of the switching architecture is closely related to the transient behavior of an equivalent system with zero input.

We shall now describe the design of both the first-order observer and the memoryless switching law $v(\cdot, \cdot)$. In the interest of space, many of the formal details regarding these designs have been omitted. The document [14] provides a complete description of the ensuing designs, and references to appropriate chapters in [14] are provided when necessary.

2.1. Design of memoryless switching law

We begin by providing a state-space description of the plant dynamics $P(s)$ of Equation (1). If the input $r(t)$ in Figure 1 is a constant for positive time (i.e. $r(t)=r$ for all $t>0$), then at any given time $t>0$, the dynamics of the plant $P(s)$ of Equation (1) can be described via[‡]

$$\begin{bmatrix} \dot{x}_1 \\ \dot{x}_2 \end{bmatrix} = \begin{bmatrix} 0 & \sqrt{a} \\ 0 & b \end{bmatrix} \begin{bmatrix} x_1 \\ x_2 \end{bmatrix} \pm \begin{bmatrix} 0 \\ \sqrt{a} \end{bmatrix} (r - x_1) \tag{3}$$

where '$\pm$' is determined as either $+$ or $-$ via the output of the memoryless switching law $v(\cdot)$. If we define the new variables $z_1(t) = x_1(t) - r$ and $z_2(t) = x_2(t)$, then it follows that the state-space

[‡]While the state-space description of this plant is not unique, it can be shown that memoryless switching laws that are designed for arbitrary minimal state-space realizations of this plant can be related through a coordinate transformation. See [14, Chapter 3] for details.

DOI: 10.1002/rnc

description equation (3) can be rewritten as follows:

$$\begin{bmatrix}\dot{z}_1\\ \dot{z}_2\end{bmatrix}=\begin{bmatrix}0 & \sqrt{a}\\ \mp\sqrt{a} & b\end{bmatrix}\begin{bmatrix}z_1\\ z_2\end{bmatrix} \tag{4}$$

From the above, we see that the zero-state response of the plant $P(s)$ to a constant input can be modeled as the zero-input response of the plant shown in Equation (4) with corresponding initial conditions $z_1(0)=x_1(0)-r$ and $z_2(0)=x_2(0)$, and output $y(t)=z_1(t)+r$. Hence, we may view the problem of designing a memoryless switching law to track a step input as a problem in which we design an asymptotically stabilizing controller in the new variables z_1 and z_2.

As an initial simplifying assumption, we shall design a memoryless switching law that has access to *both* states of the plant z_1 and z_2. Once we have arrived at a memoryless switching law $v(z_1, z_2)$ that is stabilizing, we shall discuss how to arrive at a memoryless switching law that relies, in part, on an estimate of the second state, denoted as $\hat{z}_2$, that will also achieve stability. This, in turn, will allow us to arrive at a design for a memoryless switching law in the original x_1-x_2 coordinate space.

The design of a memoryless switching law $v(z_1, z_2)$ that yields an asymptotically stable interconnected system draws upon prior work that is presented in [14, Chapter 3]. Although we shall not describe this work in full detail, we shall highlight the major results that allow us to design asymptotically stabilizing memoryless switching laws in what follows. The basic problem that is considered in [14, Chapter 3] is as follows: consider a single-input single-output, second-order LTI plant of the form

$$\dot{z}=Az+Bu$$

$$y=Cz$$

where the corresponding transfer function $P(s)=C(sI-A)^{-1}B$ is of relative degree 2. We wish to design a memoryless switching law $v(z)$ that satisfies the following conditions:

1. The range of $v(z)$ is bounded, i.e. $v(z)\in[-v_0, v_0]$ for some $v_0>0$.
2. The control law $u=v(z)y$ yields an asymptotically stable closed-loop system in the sense that $\dot{z}=(A+v(z)BC)z$ is asymptotically stable.
3. The corresponding *rate of convergence* $R(v_0)$ given by

$$R(v_0)=\min_{\|z(0)\|=1}\liminf_{T\to\infty}-\frac{1}{2T}\ln(\|z(T)\|^2)$$

is as large as possible.

The real parameter v_0 in item 1 above plays the role of the symmetric switching gain. In the problem we are investigating, $v_0=1$ since we are switching between gains of $+1$ and -1. Under certain mild assumptions on the value of v_0 along with the parameters of the matrices A, B, and C, we arrive at the following results:

1. The maximum rate of convergence, denoted by $R^*(v_0)$, is given by

$$R^*(v_0)=-\lambda_{\min}(A+v_0BC)>0 \tag{5}$$

where $\lambda_{\min}(\cdot)$ denotes the smallest eigenvalue of a square matrix.

DOI: 10.1002/rnc

2. Let w_s represent the eigenvector corresponding to the minimum eigenvalue of the matrix $A+v_0BC$ and let $\tilde{w}_s$ be a vector such that $\tilde{w}_s' w_s = 0$. Then there exists a vector $\tilde{q}$ such that the memoryless switching law

$$v(z) = \begin{cases} v_0, & z'(\tilde{w}_s\tilde{q}')z \leqslant 0 \\ -v_0, & z'(\tilde{w}_s\tilde{q}')z > 0 \end{cases} \tag{6}$$

makes the dynamical system $\dot{z} = (A + v(z)BC)z$ globally exponentially stable with rate $R^*(v_0)$.

A graphical illustration of the control law $v(z)$ in item 2 is depicted in Figure 2. Note that if the initial condition $z(0)$ lies along w_s, then, by choosing a control law with $v(w_s) = v_0$, the state trajectory will evolve as

$$z(t) = \mathrm{e}^{\lambda_{\min}(A+v_0BC)t} z(0)$$

which converges to the origin exponentially with rate $-\lambda_{\min}(A+v_0BC)$. The basic principle behind the design of the overall control law $v(z)$ is, hence, as follows: if the initial condition $z(0)$ does not initially lie along the manifold spanned by w_s, design $v(z)$ such that the state trajectory will reach this manifold in finite time. By choosing any vector q that lies 'between' w_s and w_u (which is the eigenvector corresponding to the maximum eigenvalue of $A+v_0BC$), we can find a vector $\tilde{q}$ that is normal to q such that the control law of Equation (6) achieves this goal. A sample phase portrait is illustrated in Figure 2. Here, the initial condition $z(0)$ lies in the region where $v(z) = v_0$; hence, the system dynamics initially evolve according to $\dot{z} = (A+v_0BC)z$. In finite time, the state trajectory is driven onto the manifold spanned by the vector q at which time $v(z)$ switches from v_0 to $-v_0$. The eigenvalues of matrix $A - v_0BC$ are designed to be complex valued; hence, rotation is induced, and the state trajectory is driven onto the manifold spanned by w_s in finite time. Once the state trajectory is driven onto this manifold, it remains there forevermore, and a simple calculation shows that the state trajectory converges to the origin with the rate given in Equation (5).

Note that vector q (and, correspondingly, $\tilde{q}$) is a free parameter. Therefore, the control law of Equation (6) is not unique (the interested reader is referred to [14, Chapter 3] for a discussion of ways in which one may choose to select vectors q and $\tilde{q}$). Despite this fact, although the choice of q may affect the amount of time for which the phase portrait with a given initial condition will rotate, it does *not* affect the rate of convergence of the corresponding state trajectory. Regardless of the choice of q, all state vectors become a multiple of the stable eigenvector w_s in finite time

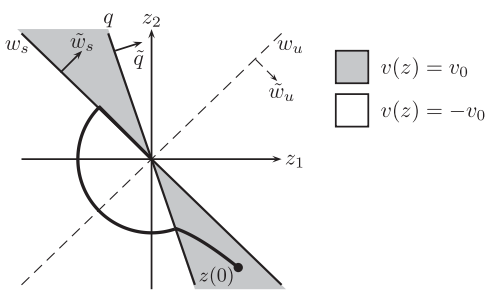

Figure 2. Graphical illustration of the switching law of Equation (6). Vector w_u represents the eigenvector corresponding to the maximum eigenvalue of matrix $(A+v_0BC)$ and $\tilde{w}_u$ is a normal vector to this eigenvector $(\tilde{w}_u' w_u = 0)$.

DOI: 10.1002/rnc

and decay with rate $-\lambda_{\min}(A+v_0BC)$ in finite time. The choice of q becomes more relevant in the presence of time delays and, in this case, one must choose q to be not too close in angle to w_s to ensure that a delay in detecting when the state trajectory crosses w_s does not cause the state trajectory to 'skip over' the region in the state space where shrinkage in the Euclidean norm of the state vector occurs (see [14, Chapter 4] for a formal description of this phenomenon).

Before proceeding further, it is important to point out that the aforementioned switching law was designed *only* with the goal of asymptotic stability with minimum convergence rate in mind; the goal of controlling overshoot and 1% settling time for a step input—the ultimate goal of this section—was never incorporated into the derivation of the above control law. Nevertheless, as we shall show here, the above controller *does* possess benefits in terms of settling time and overshoot, although these goals were not constraints in the original problem. In layman's terms, we essentially obtain these benefits for free.

Returning now to the problem at hand, we wish to design a memoryless switching law $v(z_1, z_2)$ for the system with dynamics that are described via Equation (4). Matrix $A+v_0BC$ corresponds to matrix

$$\begin{bmatrix} 0 & \sqrt{a} \\ \sqrt{a} & b \end{bmatrix} \tag{7}$$

which has eigenvector w_s and normal vector $\tilde{w}_s$ given by

$$w_s = \begin{bmatrix} -2\sqrt{a} \\ -b+\sqrt{b^2+4a} \end{bmatrix}, \quad \tilde{w}_s = \begin{bmatrix} -b+\sqrt{b^2+4a} \\ 2\sqrt{a} \end{bmatrix}$$

where w_s represents the eigenvector corresponding to the minimum eigenvalue of $A+v_0BC$. Vector $q=[0\ \ 1]'$ satisfies all the conditions stated in [14, Chapter 3]; hence, the memoryless switching law

$$v(z_1, z_2) = \begin{cases} -1, & z_1((-b+\sqrt{b^2+4a})z_1+2\sqrt{a}z_2) \leqslant 0 \\ 1, & z_1((-b+\sqrt{b^2+4a})z_1+2\sqrt{a}z_2) > 0 \end{cases} \tag{8}$$

asymptotically stabilizes the closed-loop interconnection of Figure 1 for the plant $P(s)$ of Equation (1). In terms of the original coordinates of the plant, this can be expressed equivalently as

$$v(x_1-r, x_2) = \begin{cases} -1, & (x_1-r)((-b+\sqrt{b^2+4a})(x_1-r)+2\sqrt{a}x_2) \leqslant 0 \\ 1, & (x_1-r)((-b+\sqrt{b^2+4a})(x_1-r)+2\sqrt{a}x_2) > 0 \end{cases} \tag{9}$$

Note that the asymptotic stability of the origin in z_1-z_2 coordinates is equivalent to the asymptotic stability of the point $(r, 0)$ in x_1-x_2 coordinates.

2.2. *Observer-based control and design of first-order observer*

We have designed a memoryless switching law that is asymptotically stabilizing when the full state of the plant is available. How, then, do we design a memoryless switching law that is stabilizing when only *partial* state information is available? Specifically, how do we design a control law that is stabilizing when the memoryless switching law of Equation (9) has access to only an *estimate* $\hat{x}_2$ of the true state x_2?

DOI: 10.1002/rnc

The process we use here is similar to the process of designing linear output feedback controllers for linear systems. We have already designed a 'full-state' controller, and we now need to design only an observer that produces a sufficiently accurate estimate of the plant state. Since Equation (3) implies a state-space description for $P(s)$ of the form

$$\begin{bmatrix} \dot{x}_1 \\ \dot{x}_2 \end{bmatrix} = \begin{bmatrix} 0 & \sqrt{a} \\ 0 & b \end{bmatrix} \begin{bmatrix} x_1 \\ x_2 \end{bmatrix} + \begin{bmatrix} 0 \\ \sqrt{a} \end{bmatrix} u \tag{10}$$

$$y = x_1 \tag{11}$$

we need to provide only an estimate of the state $x_2(t)$. The design of a partial observer is an exercise in linear systems theory, the details of which can be found in [14, Chapter 4]. One observer that produces an estimate $\hat{x}_2(t)$ of the state $x_2(t)$ is given by

$$\dot{w}(t) = (b - l\sqrt{a})w + l(b - l\sqrt{a})y + \sqrt{a}u \tag{12}$$

$$\hat{x}_2(t) = w(t) + ly(t) \tag{13}$$

where $l \in \mathbf{R}$ is a free parameter. It can be shown that the dynamics of the error $d(t) = x_2(t) - \hat{x}_2(t)$ evolve according to

$$\dot{d} = (b - l\sqrt{a})d$$

which implies that $\hat{x}_2(t) \to x_2(t)$ exponentially whenever $l > b/\sqrt{a}$.

Our overall memoryless switching law now takes the following form:

$$v(x_1 - r, \hat{x}_2) = \begin{cases} -1, & (x_1 - r)((-b + \sqrt{b^2 + 4a})(x_1 - r) + 2\sqrt{a}\hat{x}_2) \leqslant 0 \\ 1, & (x_1 - r)((-b + \sqrt{b^2 + 4a})(x_1 - r) + 2\sqrt{a}\hat{x}_2) > 0 \end{cases} \tag{14}$$

One can prove that the overall interconnected system consisting of the observer equation (12) and (13) and memoryless switching law equation (14) is both asymptotically and finite $L2$ gain stable, but the proof of these statements is lengthy and is omitted due to space constraints. The interested reader is referred to [14, Chapter 4] for complete proofs of these statements.

2.3. Step response performance of switching architecture

We are now ready to describe some of the qualitative attributes of the step response of the switching architecture of Figure 1 for plants $P(s)$ of the form of Equation (1), namely the 1% settling time and overshoot of the unit step response. To begin, we first note that, under the assumption of zero initial state, the output of the observer $\hat{x}_2(t)$ is perfect, i.e. $\hat{x}_2(t) = x_2(t)$ for all $t \geqslant 0$. Hence, in computing the step response, we may ignore the observer entirely and treat the problem as if the switching law has full state access.

We shall first compute an expression for the 1% settling time T_s of the step response. Note that this can be represented in terms of the variable z_1 of Equation (4) as the smallest time $T_s > 0$ such that

$$|z_1(t)| \leqslant 0.01 \quad \forall t \geqslant T_s$$

DOI: 10.1002/rnc

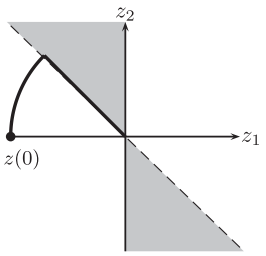

Figure 3. Example transient response in z coordinates for a plant $P(s)$ of the form of Equation (1) controlled by the switching architecture of Figure 1.

For a unit step input, the initial condition in z coordinates is $z(0)=[-1\ \ 0]$. Since $v(z)$ is initially 1, a simple calculation shows that the state evolution is initially given via

$$z(t)=\mathrm{e}^{(b/2)t}\begin{bmatrix} -\cos\beta t+\dfrac{b}{\sqrt{4a-b^2}}\sin\beta t \\ \dfrac{2\sqrt{a}}{\sqrt{4a-b^2}}\sin\beta t \end{bmatrix} \tag{15}$$

where $\beta=\frac{1}{2}\sqrt{4a-b^2}$. The state $z(t)$ evolves in the above manner until a certain time which we shall denote T_1 at which point $z(t)$ crosses the stable eigenvector w_s, which can be expressed as $z(T_1)=\gamma w_s$ for some $\gamma\in\mathbf{R}$. Simple calculations show that this time T_1 is given by

$$T_1=\frac{2}{\sqrt{4a-b^2}}\operatorname{arccot}\left(\frac{2b+\sqrt{b^2+4a}}{\sqrt{4a-b^2}}\right) \tag{16}$$

For times $t\geqslant T_1$, the state then evolves according to

$$z(t)=\mathrm{e}^{\delta(t-T_1)}z(T_1) \tag{17}$$

where $\delta=\frac{1}{2}(b-\sqrt{b^2+4a})$ is the stable eigenvalue of the matrix in Equation (7). We find that, for $t>T_1$,

$$z_1(t)=-\frac{1}{\sqrt{2}}\mathrm{e}^{bT_1/2}\,\mathrm{e}^{\delta(t-T_1)} \tag{18}$$

It, hence, follows that the 1% settling time T_s is the value of t in Equation (18) for which $z_1(t)=-0.01$, which can be expressed explicitly as

$$T_\mathrm{s}=\frac{1}{\delta}\ln\left(\frac{\sqrt{2}}{100}\right)+\left(1-\frac{b}{2\delta}\right)T_1 \tag{19}$$

A sample phase portrait in z coordinates is depicted in Figure 3. The portion of the phase portrait which lies along the depicted circular arc represents the initial T_1 seconds of evolution where the state is described by Equation (15), while the portion that lies along the stable manifold is the portion that is described by Equation (17). The phase portrait indicates that $z_1(t)<0$ for all $t\geqslant 0$. This implies that $y(t)=z_1(t)+r<r$ for all $t\geqslant 0$, which, in turn, implies that the step response

DOI: 10.1002/rnc

has no overshoot. Indeed, with the constraint $a \geqslant b^2$ in place, this statement is true. Examining the expression for $z_2(t)$ in Equation (15), we see that $z_2(t) \geqslant 0$ for $0 \leqslant t \leqslant \pi/\beta$. Because $\dot{z}_1 = \sqrt{a} z_2$, it follows that $z_1(t)$ is increasing for $0 \leqslant t \leqslant \pi/\beta$. Now, since $z_1(T_1) = -\exp(bT_1/2)/\sqrt{2} < 0$, it follows that $z_1(t) < 0$ for $0 \leqslant t \leqslant T_1$. Moreover, since $z_1(t)$ is given by Equation (18) for $t \geqslant T_1$, it follows that $z_1(t) < 0$ for all $t \geqslant 0$; hence, $y(t)$ exhibits no overshoot.

2.4. Design example: double integrator

For illustrative purposes, we shall now examine the characteristics of the step response when the switching architecture of Figure 1 is used to control a double integrator ($P(s) = 1/s^2$) with canonical state-space description

$$\begin{bmatrix} \dot{x}_1 \\ \dot{x}_2 \end{bmatrix} = \begin{bmatrix} 0 & 1 \\ 0 & 0 \end{bmatrix} \begin{bmatrix} x_1 \\ x_2 \end{bmatrix} + \begin{bmatrix} 0 \\ 1 \end{bmatrix} u$$
$$y = x_1$$

In order to specify a controller, we need to supply two objects:

- A first-order observer that provides an estimate $\hat{x}_2(t)$ of the state $x_2(t)$.
- A memoryless switching law $v(\cdot)$.

2.4.1. Observer design. For the double integrator, the dynamics of $w(t)$ of Equation (12) are given by

$$\dot{w} = -lw - l^2 y + u$$

from which it immediately follows that any $l > 0$ will achieve stable error dynamics. For simplicity, we choose $l = 1$. Our observer is, therefore, given by

$$\dot{w} = -w - y + u$$
$$\hat{x}_2 = w + y$$

2.4.2. Supervisor design. Following the recipe of the previous section, for a constant input r, if we define the variables $z_1 = x_1 - r$, $z_2 = x_2$, their evolution at any time t can be described via

$$\begin{bmatrix} \dot{z}_1 \\ \dot{z}_2 \end{bmatrix} = \begin{bmatrix} 0 & 1 \\ \pm 1 & 0 \end{bmatrix} \begin{bmatrix} z_1 \\ z_2 \end{bmatrix}$$

where, again, either '+' or '−' is selected via the memoryless switching law. When the lower left-hand element of the matrix above is $+1$, the stable eigenvector w_s and the corresponding vector $\tilde{w}_s$ are given by

$$w_s = \begin{bmatrix} 1 \\ -1 \end{bmatrix}, \quad \tilde{w}_s = \begin{bmatrix} 1 \\ 1 \end{bmatrix}$$

DOI: 10.1002/rnc

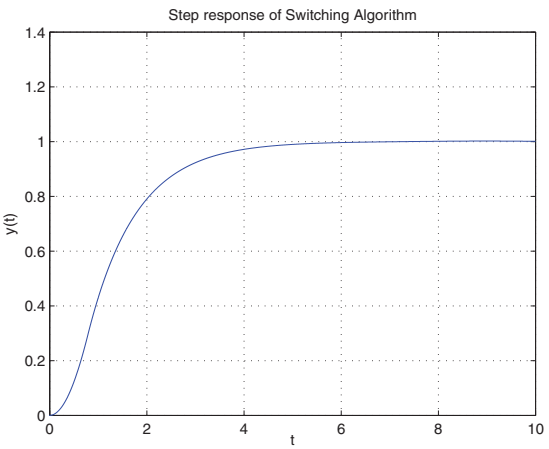

Figure 4. Step response of double integrator controlled by the switching architecture of Figure 1.

Hence, we choose as our 'full-state' supervisor

$$v(z_1, z_2) = \begin{cases} -1, & z_1(z_1+z_2) \leqslant 0 \\ 1, & z_1(z_1+z_2) > 0 \end{cases}$$

The supervisor that assumes access only to e and $\hat{x}_2$ is then given by

$$v(e, \hat{x}_2) = \begin{cases} 1, & e(-e+\hat{x}_2) \leqslant 0 \\ -1, & e(-e+\hat{x}_2) > 0 \end{cases}$$

2.4.3. Results. The step response using the above observer and supervisor is depicted in Figure 4. As proved in the previous section, the step response exhibits no overshoot. The 1% settling time for the double integrator (corresponding to the values $a=1, b=0$) is $T_s = \pi/4 + \ln(100/\sqrt{2}) \approx 5.04$.

3. COMPARISON: FIRST-ORDER LTI CONTROL

The main objective of this exposition is to obtain an understanding of how the switching architecture discussed in the last section performs compared with other more traditional forms of control. In this section, we wish to compare the performance of the step response that is achieved via our switching architecture with the performance of the set of step responses, which are achievable via first-order LTI control. The specific architecture we will consider is the so-called *servo* configuration shown in Figure 5 where, for the present time, we restrict $K(s)$ to be a first-order LTI system:

$$K(s) = k\frac{s+c}{s+d} \tag{20}$$

with $k, c, d \in \mathbf{R}$.

As a first goal, we shall undergo the process of designing a first-order controller $K(s)$ for the specific case where the plant is a double integrator $P(s) = 1/s^2$. This will allow us to quantitatively

DOI: 10.1002/rnc

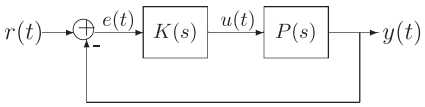

Figure 5. Servo control architecture.

compare the performance of the switching architecture with the achievable performance of a first-order LTI controller for a specific case study and, as we shall see, provide some insight into the performance capabilities of the switching architecture. In a later section, we shall then extend the results for this specific example to a subclass of the set of plants $P(s)$ of the form

$$P(s)=\frac{a}{s(s-b)}$$

for which we shall be able to make a somewhat more general performance statement.

The way in which we shall compare the performance of the two architectures will be to determine the *achievability region* of percentage overshoot and 1% settling time that is obtainable via first-order LTI control. More specifically, if we denote by M and T the percentage overshoot and 1% settling time, respectively, of a particular stabilizing first-order LTI controller $K(s)$, then we wish to determine the set of ordered pairs (M,T), which result as we allow $K(s)$ to range over an entire class of first-order LTI controllers. The reason as to why we wish to compute such an achievability region rather than trying to compute the controller that produces the minimal overshoot and/or the minimal 1% settling time is to gather information about potential trade-offs between percentage overshoot and settling time.

3.1. Preliminaries: controller constraints

Note that in the above description we said that we wish to determine the achievability region for a *class* of first-order controllers. Indeed, if we do not impose some limitations on our controller sets, we may potentially allow ourselves to use controllers that exhibit 'unreasonable' behavior. The first constraint that we shall impose is that the control signal $u(t)$ be bounded for all $t\geqslant 0$. The second constraint that we shall impose is related to the controller's ability to reject disturbances present at the input of the plant $P(s)$. Specifically, if one considers the augmented block diagram of the servo configuration shown in Figure 6 in which an exogenous input $w(t)$ is present at the input of the plant $P(s)$, we wish to place a bound on the closed-loop $L2$ gain from the plant input $w(t)$ to the plant output $y(t)$. That is, for some constant $C>0$, we wish to search over only those first-order controllers $K(s)$ for which the corresponding closed-loop transfer function from w to y $H_{wy}(s)$ satisfies $\|H_{wy}\|_\infty\leqslant C$, where $\|\cdot\|_\infty$ represents the H-infinity norm of a stable transfer function.

To understand the origins of the $L2$ gain constraint, we will consider a simple example.

Example 3.1

For the block diagram of Figure 6 with plant $P(s)=1/s^2$, consider the controller $K(s)$ given by

$$K(s)=\frac{\alpha^2 s}{(s+2\alpha)}$$

DOI: 10.1002/rnc

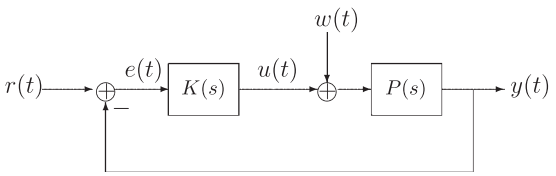

Figure 6. Servo architecture with plant input disturbance $w(t)$.

where $\alpha>0$ is a parameter. For this choice of $K(s)$, the closed-loop transfer function from $r(t)$ to $y(t)$, $H_{ry}(s)$, is given by

$$H_{ry}(s)=\left(\frac{\alpha}{s+\alpha}\right)^2$$

It can be shown using standard tools from linear systems theory that the step response of $H_{ry}(s)$ exhibits no overshoot for any $\alpha>0$ and has 1% settling time that tends to 0 as $\alpha\to\infty$. Although this may initially indicate that the work of the previous section was for naught, note that this controller is *not* a stabilizing controller due to the unstable pole–zero cancellation introduced at $s=0$. Indeed, the transfer function from $w(t)$ to $y(t)$, $H_{wy}(s)$, is given by

$$H_{wy}(s)=\frac{s+2\alpha}{s(s+\alpha)^2}$$

which has an unstable pole at $s=0$. Because the $L2$ gain of an LTI system is equal to the H-infinity norm of the corresponding transfer function, we see that the $L2$ gain from $w(t)$ to $y(t)$ is infinite for this choice of controller. Furthermore, any effort to remove this effect by perturbing the controller to be of the form

$$K(s)=\frac{\alpha^2(s+\varepsilon)}{(s+2\alpha)}$$

where $\varepsilon>0$ is small will lead a closed-loop transfer function $H_{wy}(s)$, which satisfies the constraint

$$\|H_{wy}(s)\|_\infty\geqslant|H_{wy}(0)|=\frac{2}{\alpha\varepsilon}$$

which shows that the $L2$ gain from $w(t)$ to $y(t)$ for small ε can still be very large.

The above example is indicative that there may be a trade-off between step response performance and disturbance rejection at the input to the plant. Since systems that have low disturbance rejection properties are undesirable, we wish to search over only those controllers that have sufficiently low disturbance rejection properties. The $L2$ gain provides a convenient way to formally quantify disturbance rejection so that we can make a proper mathematical comparison.

In forming a comparison between the performance we can achieve via first-order LTI control and the performance of the switching architecture we have constructed, we must take care to ensure the same set of constraints for both architectures. Because we are considering only a single design within the framework of the switching architecture, the values of these constraints are determined *de facto*. In what follows, we shall first determine the numerical values of these bounds for the

DOI: 10.1002/rnc

switching architecture. Once we have done this, we shall then numerically compute the set of achievable pairs of 1% settling time and overshoot for all first-order controllers $K(s)$ which satisfy the same numerical bounds on the peak control value and the $L2$ gain constraint.

3.1.1. Switching architecture: peak control bound. As mentioned in the process of designing the switching architecture, the choice of switching between gains of $+1$ and -1 was related to the fact that, in the end, we desired to constrain the peak control value to be 1, i.e. we wished to impose the constraint that $|u(t)|\leqslant 1$ for all $t>0$, a fact we now show.

First, note that $|u(t)|=|r(t)-y(t)|=|e(t)|$; hence, it suffices to show that $|e(t)|$ never exceeds 1 when $r(t)$ is a unit step input. Now, we have already shown that the output $y(t)$ is monotonically increasing for all $t>0$ and satisfies the constraints

$$y(0)=0, \quad \lim_{t\to\infty} y(t)=1$$

It then follows that $e(t)$ is monotonically decreasing for $t>0$ and satisfies the conditions

$$e(0)=1, \quad \lim_{t\to\infty} e(t)=0$$

Hence, $0\leqslant e(t)\leqslant 1$ for all $t>0$, and it follows that $|u(t)|\leqslant 1$ for all $t\geqslant 0$.

3.1.2. Switching architecture: $L2$ gain from $w(t)$ to $y(t)$. Unlike the peak control bound, the $L2$ gain from w to y is not plant independent. Furthermore, as is the case with most nonlinear systems, the $L2$ gain cannot be computed exactly. Nevertheless, one can compute upper bounds on the $L2$ gain from w to y by using the $\mathscr{S}$-procedure and searching over piecewise quadratic storage functions [14]. For the case where the plant is a double integrator, one can numerically show that 8.38 is an upper bound on the $L2$ gain from $w(t)$ to $y(t)$.

3.2. First-order controller class

Now that we have computed the constraints that we wish to impose on the closed-loop system of Figure 6, we are in the position of being able to compute the constraints on the associated first-order controller $K(s)$ of the form

$$K(s)=k\frac{s+c}{s+d}$$

We shall first determine constraints on the value of k that are induced by the peak control bound and will then determine constraints on the values of c and d imposed by the constraint on the $L2$ gain from w to y.

3.2.1. Peak control bound. When $P(s)=1/s^2$ and $K(s)$ is as shown above, the closed-loop transfer function from $r(t)$ to $u(t)$ in the servo configuration of Figure 6 is given by

$$H_{ru}(s)=\frac{ks^2(s+c)}{s^3+ds^2+ks+kc} \tag{21}$$

When the input $r(t)$ is a unit step with Laplace transform $R(s)=1/s$, the initial value theorem implies us that $u(0)=\lim_{s\to\infty} sU(s)=k$. Hence, if we wish to constrain the peak value of the control to be less than 1 for all $t\geqslant 0$, it follows that $|k|\leqslant 1$. Moreover, by examining the denominator

DOI: 10.1002/rnc

of Equation (21), the Routh criterion constrains k to be positive. Hence, we consider only values of k for which $0<k\leqslant 1$.

As it turns out, the value of k which yields the 'best' performance is the value $k=1$. We formalize this in the following statement.

Proposition 3.1
Consider the system of Figure 6 where $P(s)=1/s^2$ and where $K(s)$ is a first-order controller of the form of Equation (20):

$$K(s)=k\frac{s+c}{s+d}$$

with $0<k<1$, and denote by M and T the percentage overshoot and 1% settling time of the unit step response $y(t)$. Suppose that $K(s)$ satisfies the constraint

$$\left\| \frac{P(s)}{1+P(s)K(s)} \right\|_\infty <\gamma$$

for some $\gamma>0$. Then the following statements are true:

1. The peak control value to a unit step input is equal to k.
2. The controller

$$\tilde{K}(s)=\frac{s+c/\sqrt{k}}{s+d/\sqrt{k}}$$

satisfies the constraint

$$\left\| \frac{P(s)}{1+P(s)\tilde{K}(s)} \right\|_\infty <\gamma$$

Moreover, the peak control effort $u(t)$ in response to a unit step input with the controller $\tilde{K}(s)$ in place of $K(s)$ is equal to 1, and the percentage overshoot and 1% settling time of the corresponding step response $y(t)$ are given by M and $T\sqrt{k}$, respectively.

The proof of Proposition 3.1 is rather technical and is given in the Appendix. In layman's terms, the result of the proposition is as follows: if we can find a controller with peak gain strictly less than 1 for which the closed-loop $L2$ gain from $w(t)$ to $y(t)$ (characterized by the H_∞ norm constraint) is less than a certain value γ, then we can always find another controller for which the peak gain is exactly equal to 1 and for which the $L2$ gain constraint is still satisfied. Moreover, this new controller has a percentage overshoot that is exactly the same as the original controller but with a 1% settling time that is reduced by a factor of $\sqrt{k}$. Hence, it is sufficient to search over the set of controllers $K(s)$ of the form of Equation (20) with $k=1$.

3.2.2. L2 gain bound. Based on the results of Proposition 3.1, it is sufficient to limit the set of controllers over which we search to those which take the form

$$K(s)=\frac{s+c}{s+d} \tag{22}$$

DOI: 10.1002/rnc

Hence, the set of controllers that we wish to examine are those for which the closed-loop $L2$ gain from $w(t)$ to $y(t)$ in Figure 6 is bounded above by $\gamma = 8.38$. This requirement can be expressed as searching over the set of $(c, d) \in \mathbf{R}^2$ for which

$$\|H_{wy}(s)\|_\infty \triangleq \left\| \frac{s+d}{s^3+ds^2+s+c} \right\|_\infty \leqslant \gamma \tag{23}$$

As we shall show now, the set of pairs $(c, d) \in \mathbf{R}^2$ that satisfy the condition of Equation (23) for any $\gamma > 0$ lies in a bounded set. Although it is difficult to analytically compute the exact set of pairs (c, d) that satisfy the above condition, we shall find an outer approximation of this region which will allow us to be able to estimate the achievability region that we wish to calculate.

To begin, define

$$W = \{(c, d) \in \mathbf{R}^2 : c > 0, d > 0, d > c\}$$

The set W is the set of $(c, d) \in \mathbf{R}^2$ for which all the roots of the polynomial $s^3 + ds^2 + s + c$ lie in the open left half-plane [23] and, hence, represents the domain for which the H_∞ norm of Equation (23) is well defined. Let V_γ be defined by the condition

$$V_\gamma = \{(c, d) \in W : \|H_{wy}(s)\|_\infty \leqslant \gamma\} \tag{24}$$

for some $\gamma > 0$. It is precisely the set V_γ that we wish to show is bounded. To do so, we compute $|H_{wy}(j\omega)|$ of Equation (23) at a few select frequencies. First, note that $|H_{wy}(0)| = d/c$. If the infinity norm of $H_{wy}(s)$ is to be less than some value γ, then $|H_{wy}(j\omega)|$ must be less than γ for every frequency ω, which implies that $|H_{wy}(0)| \leqslant \gamma$ or that

$$d \leqslant \gamma c \tag{25}$$

If we now compute $|H_{wy}(j\omega)|$ at $\omega = 1$, we have

$$|H(j)| = \left| \frac{j+d}{c-d} \right| \geqslant \frac{1}{1 - \dfrac{c}{d}}$$

Recognizing that the rightmost inequality must be less than or equal to γ yields the condition

$$d \geqslant \frac{\gamma}{\gamma - 1} c \tag{26}$$

Further analysis at $\omega = 1$ along with analysis at $\omega = \sqrt{c/d}$ yields the following additional bounds:

$$d \geqslant \frac{1}{\gamma - 1} \tag{27}$$

$$d \leqslant \gamma \tag{28}$$

A graphical depiction of the region described by inequalities (25)–(28) is shown in Figure 7. Note that, in general, the region V_γ of Equation (24) is *not* the region that is defined by the inequalities above. Rather, V_γ is a subset of this region.

DOI: 10.1002/rnc

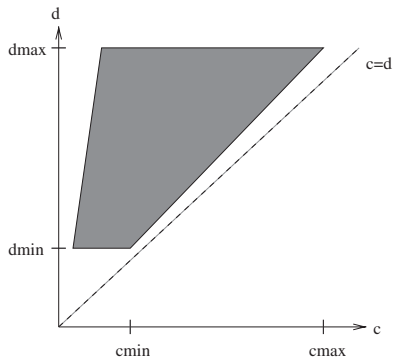

Figure 7. Region described by inequalities (25)–(28), with $c_{\min} = 1/(\gamma^2 - \gamma)$, $c_{\max} = \gamma - 1$, $d_{\min} = 1/(\gamma - 1)$, and $d_{\max} = \gamma$.

3.3. Computation of achievable percentage overshoot and 1% settling time pairs

We have now limited the process of computing the set of achievable pairs (M, T) of percentage overshoot and 1% settling time pairs to a search over a bounded region of $\mathbf{R}^2$. Because overshoot and settling time are not analytically parameterizable, we attempt to compute an approximation of the achievable set of pairs (M, T) by finely gridding the bounded region of Figure 7. For each grid point (c_i, d_j) in this region, we first determine whether $(c_i, d_j) \in V_\gamma$, i.e. whether the corresponding closed-loop transfer function $H_{wy}(s)$ of Equation (23) satisfies the imposed norm-bound condition. Once we have found the set of points in the grid which lie in V_γ, we simulate the corresponding unit step response in MATLAB and measure the percentage overshoot and 1% settling time for each grid point in V_γ.

The results of this gridding process are shown in Figure 8. The overshoot and 1% settling time pairs that are achievable via first-order LTI control under the given peak control and $L2$ gain constraints are depicted by the '$\times$' symbols, whereas the performance of the switching architecture that we designed in Section 1 is shown via the circle at the bottom of the figure for comparison. Note that the LTI control does exhibit a trade-off between percentage overshoot and 1% settling time; the minimal percentage overshoot of 26% has a settling time of 17.5 s, while the minimal 1% settling time of 10.5 s has a corresponding overshoot of 37%. A plot of the step response with minimal percentage overshoot and a plot of the step response with minimal 1% settling time are shown in Figure 9.

Although it is impossible to obtain the exact minimal values of percentage overshoot and 1% settling time via a gridding procedure, Figure 8 is clearly indicative of a finite gap between the minimal 1% settling time and minimal percentage overshoot that can be achieved via first-order LTI control *vs* what can be achieved via the switching algorithm designed in Section 1.

3.4. First-order LTI control for other plants

We can perform similar comparisons between the performance of the switching architecture and the performance that is achievable via first-order LTI control for plants other than the double

DOI: 10.1002/rnc

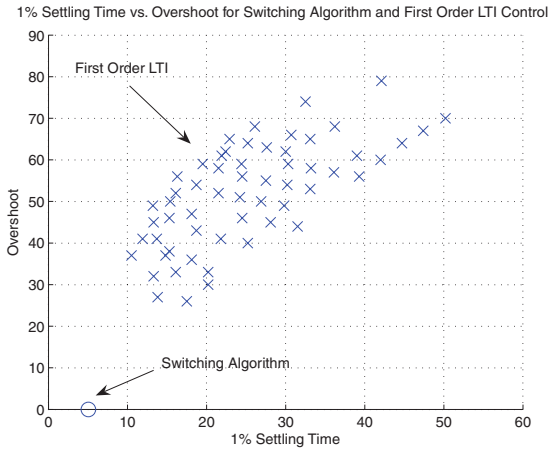

Figure 8. Achievable percentage overshoot and 1% settling time pairs that can be achieved via first-order LTI control for the given peak control and $L2$ gain constraints (shown by '$\times$' in the picture). The performance of the switching architecture is shown via the circle at the bottom of the figure for comparison.

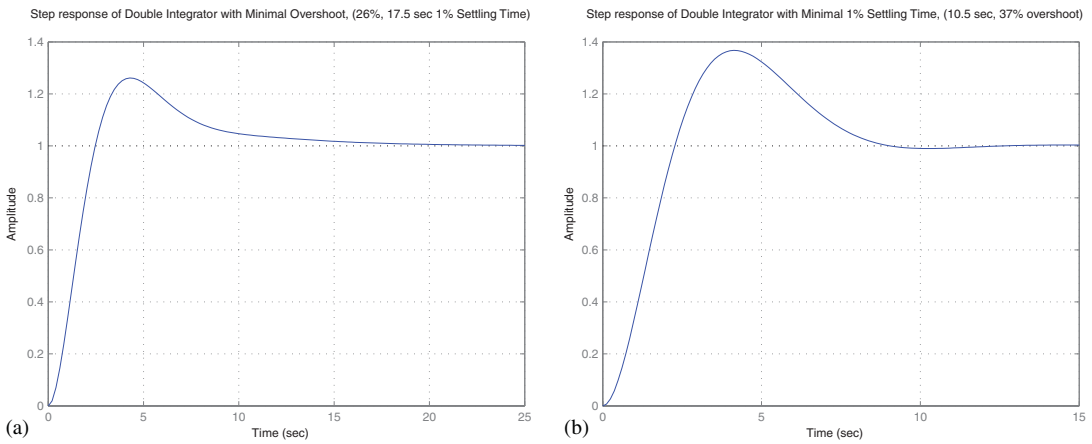

Figure 9. Step responses of double integrator which achieve minimal overshoot and minimal 1% settling time subject to the peak control value and $L2$ gain-bound constraints given in this section: (a) minimal overshoot and (b) minimal 1% settling time.

integrator, as well. Here, we shall consider two additional plants:

$$P_1(s) = \frac{100}{s(s+1)}, \quad P_2(s) = \frac{100}{s(s-1)}$$

Informally, the above plants are 'close' to a double integrator in the sense that the corresponding values of a and b for each plant satisfy the constraint that $a \gg b^2$ (in both cases $a/b^2 = 100$). In a slightly more formal setting, we can view the transfer function $P(s)$ of Equation (1) as a

DOI: 10.1002/rnc

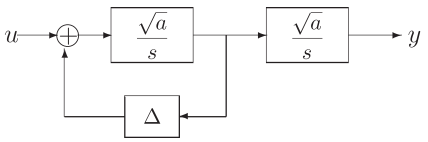

Figure 10. Realization of transfer function $P(s)$ of Equation (1) where $\Delta = b/\sqrt{a}$.

perturbation of a double integrator in the following manner: the transfer function $P(s)$ can be realized via the block diagram of Figure 10 where $\Delta = b/\sqrt{a}$. The case when $a \gg b^2$ can, therefore, be viewed as a case where Δ is small in Figure 10.

Returning now to our performance comparison, we design switching controllers for the plants $P_1(s)$ and $P_2(s)$ using the algorithm presented in Section 1 and then evaluate the performance of a first-order LTI controller subject to the same peak gain condition $|u(t)| \leqslant 1$ for all $t \geqslant 0$ and a similar $L2$ gain-bound condition (where, obviously, the $L2$ gain bounds are the bounds that we numerically compute for the switching architectures that control $P_1(s)$ and $P_2(s)$, respectively). The results for $P_1(s)$ and $P_2(s)$ are shown in Figures 11 and 12, respectively. Part (a) of each figure shows the step response that is obtained via the switching algorithm presented in Section 1, whereas parts (b) and (c) of each figure show the step response with a first-order LTI controller $K(s)$ placed in a servo configuration of Figure 5 that achieves minimal overshoot and minimal 1% settling time, respectively.

It is difficult to make general statements about a class of systems for which the use of the switching architecture presented in this section has clear benefits over using a first-order LTI controller. Part of this is simply due to the fact that quantities such as percentage overshoot and 1% settling time are not quantities that are, in general, easily analytically parameterizable. Nevertheless, although we cannot currently provide a broad general class, we can offer the following weak generalization.

Proposition 3.2
Consider a plant $P(s)$ and a controller $K(s)$ of the form

$$P(s) = \frac{a}{s(s-b)}, \quad K(s) = k\frac{s+c}{s+d}$$

with $a > 0$, $k > 0$, $b, c, d \in \mathbf{R}$, and define

$$H_1(s) = \frac{K(s)}{1+P(s)K(s)} \quad H_2(s) = \frac{P(s)K(s)}{1+P(s)K(s)}$$

Suppose that the following three properties hold:

1. The step response $u(t)$ of system $H_1(s)$ satisfies the condition $|u(t)| \leqslant 1$ for all $t \geqslant 0$.
2. $\|H_2(s)\|_\infty$ is finite and satisfies $\|H_2(s)\|_\infty \leqslant \gamma$ for some $\gamma > 0$.
3. The unit step response $s(t)$ of $H_2(s)$ has percentage overshoot M and 1% settling time T.

Then the transfer functions $\tilde{H}_1(s)$ and $\tilde{H}_2(s)$ given by

$$\tilde{H}_1(s) = \frac{\tilde{K}(s)}{1+\tilde{P}(s)\tilde{K}(s)}, \quad \tilde{H}_2(s) = \frac{\tilde{P}(s)\tilde{K}(s)}{1+\tilde{P}(s)\tilde{K}(s)}$$

DOI: 10.1002/rnc

with

$$\tilde{P}(s)=\frac{a\alpha^2}{s(s-b\alpha)}, \quad \tilde{K}(s)=k\frac{s+c\alpha}{s+d\alpha}$$

for some $\alpha>0$ satisfy the following conditions.

1. The step response $\tilde{u}(t)$ of system $\tilde{H}_1(s)$ satisfies the condition $|\tilde{u}(t)|\leqslant 1$ for all $t\geqslant 0$.
2. $\|\tilde{H}_2(s)\|_\infty$ is finite and satisfies $\|\tilde{H}_2(s)\|_\infty\leqslant\gamma$.
3. The unit step response $\tilde{s}(t)$ of $\tilde{H}_2(s)$ has percentage overshoot M and 1% settling time T/α.

The proof of this statement is very similar to the second part of the proof of Proposition 3.1 and is left to the reader.

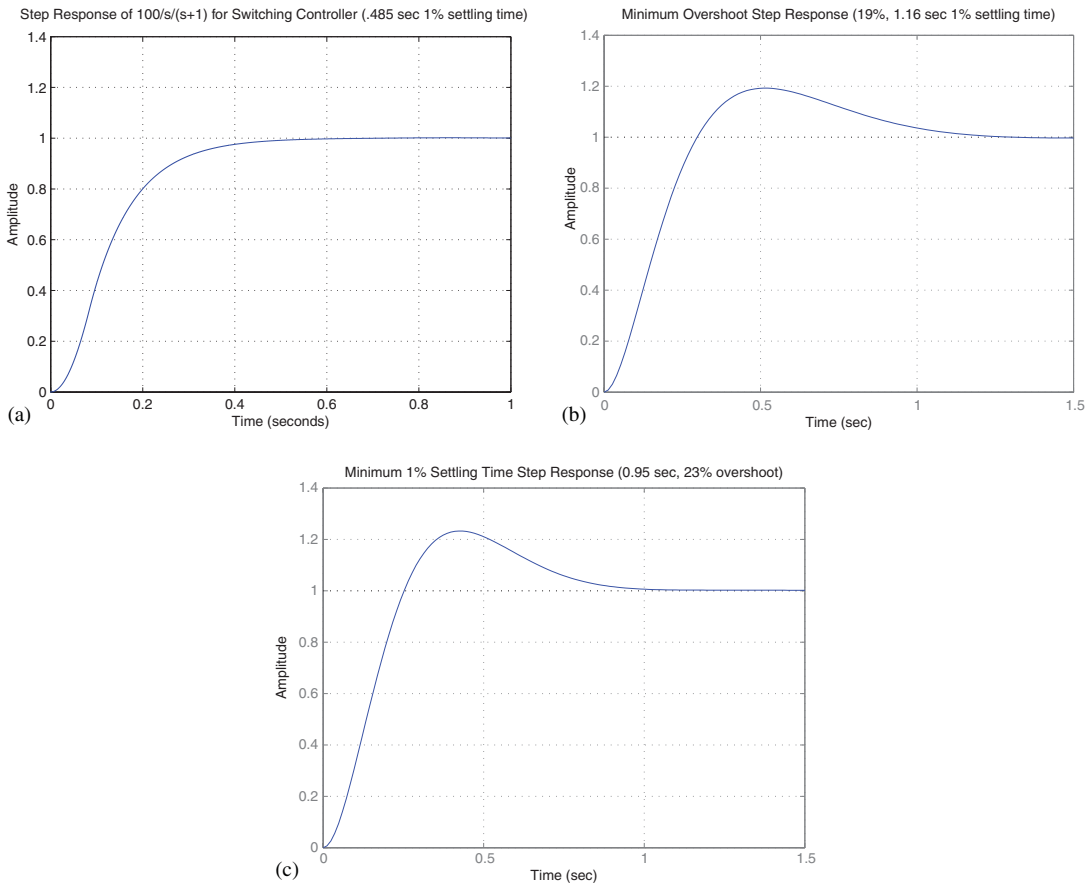

Figure 11. Step responses for $P_1(s)=100/s(s+1)$: (a) switching algorithm step response (0.485 s 1% settling time); (b) minimum overshoot with first-order LTI control (19% overshoot, 1.16 s 1% settling time); and (c) minimum 1% settling time with first-order LTI control (0.95 s 1% settling time, 23% overshoot).

DOI: 10.1002/rnc

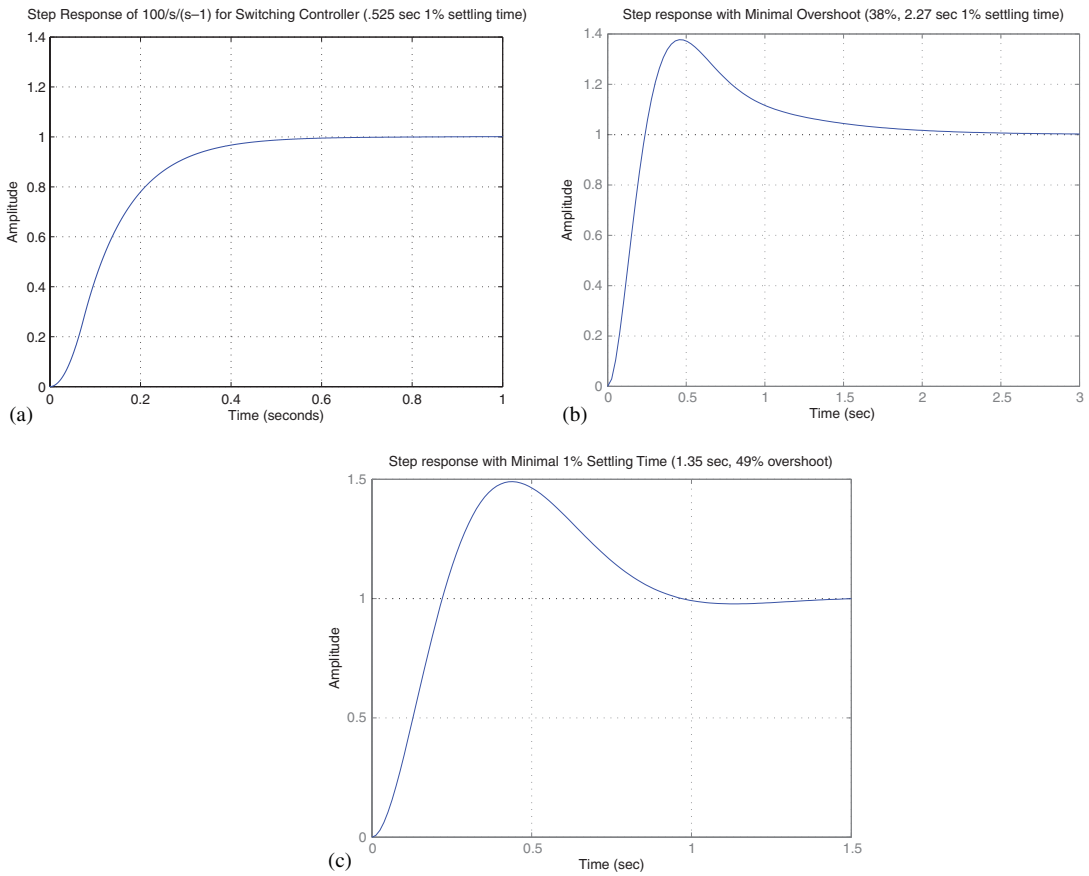

Figure 12. Step responses for $P_2(s) = 100/s(s-1)$: (a) switching algorithm step response (0.525 s 1% settling time); (b) minimum overshoot with first-order LTI control (38% overshoot, 2.27 s 1% settling time); and (c) minimum 1% settling time with first-order LTI control (1.35 s 1% settling time, 49% overshoot).

Proposition 3.2 implies us that, in optimizing for performance in terms of percentage overshoot and/or 1% settling time for a single plant, we effectively compute the optimal percentage overshoot and/or 1% settling time for an entire *class* of plants. For example, consider the plant

$$P_3(s) = \frac{1}{s(s-0.1)}$$

which is related to the plant $P_2(s)$ above via $P_3(s) = P_2(10s)$. Using the result of Proposition 3.2 for $\alpha = 0.1$, we conclude that, since the minimum achievable overshoot using first-order control for $P_2(s)$ was measured to be 38%, the minimum achievable overshoot using first-order control for $P_3(s)$ is also 38%. Moreover, since the minimum achievable 1% settling time was measured to be 1.35 s for $P_2(s)$, we conclude that the minimum achievable 1% settling time for $P_3(s)$ is 13.5 s. In general, if we know that the minimal percentage overshoot and 1% settling time for a plant $P(s)$

DOI: 10.1002/rnc

are given by M and T, respectively, then the minimal percentage overshoot and settling time of $P(s/\alpha)$ are given by M and T/α, respectively.

Now, if we denote by $T_s(P(s))$ the 1% settling time of the plant $P(s)$ that is achieved via the switching architecture of Figure 1, of Equation (19), then a simple calculation shows that $T_s((P(s/\alpha))=(1/\alpha)T_s(P(s))$. Hence, we can conclude that the *ratio* of the settling time achievable via first-order LTI control for a plant $P(s/\alpha)$ to that achievable by the switching architecture is constant for all $\alpha>0$. Hence, if a given plant $P(s)$ exhibits performance benefits in terms of 1% settling time and percentage overshoot with the switching controller in place *vs* that which can be achieved via first-order control, then the same benefits exist for the entire *class* of plants $P(s/\alpha)$ for all $\alpha>0$.

4. COMPARISON: HIGHER-ORDER LTI CONTROL

In this section, we would like to compare the performance of the switching architecture of Section 1 with certain fundamental performance limits of LTI control. Specifically, we would like to compare the 1% settling time of the switching controller for a given plant $P(s)$ of Equation (1) with the 1% settling time that can be achieved via a rational LTI controller $K(s)$ connected in the servo configuration of Figure 5 where $K(s)$ is of unconstrained order.

We shall derive bounds on the ratio of the 1% settling time achievable via the switching architecture *vs* that which is achievable via LTI control by first examining two *time-optimal* control problems. That is, we shall initially remove the restriction that the control input $u(t)$ must be the output of an LTI feedback interconnection and derive a lower bound on the 1% settling time that can be achieved by searching over all control inputs $u(t)$ with $|u(t)|\leqslant 1$ for all $t\geqslant 0$. We shall first derive a weak (conservative) lower bound on the 1% settling time achievable via bounded control to establish a formal bound on the ratio of the two settling times (switching algorithm *vs* bounded control input) and then present an approximate lower bound that, in many cases, yields a more accurate ratio.

Once we have provided the above bounds, we shall examine a method of designing LTI controllers that minimize 1% settling time with less than 1% overshoot (we shall see that this extra constraint on overshoot does not affect our ability to obtain close-to-optimal 1% settling times). As we shall see, this problem can be formulated as an infinite-dimensional linear programming problem that can be solved numerically using standard software packages. We shall examine the method for several plants to investigate the order of a controller $K(s)$ which achieves close-to-optimal performance as a function of the plant parameters a and b.

4.1. Time-optimal control, part I: bounds derived from rise time

We begin with two definitions that we shall encounter frequently in this section:

Definition 4.1
The *ε-settling time* T_ε of a real-valued signal $y(t)$ is the smallest value of $T_\varepsilon>0$ such that

$$|y(t)-1|\leqslant\varepsilon \quad \forall t\geqslant T_\varepsilon$$

If no value of T_ε exists that satisfies the above constraint, then $T_\varepsilon=\infty$.

DOI: 10.1002/rnc

Definition 4.2
The *ε-rise time* T_r of a real-valued signal $y(t)$ is the smallest value of $T_r>0$ such that

$$y(T_r)=1-\varepsilon$$

If no value of T_r exists that satisfies the above constraint, then $T_r=\infty$.

According to Definition 4.1, the 1% settling time of a signal $y(t)$ is an ε-settling time with $\varepsilon=0.01$. It is clear from the above definitions that any real-valued signal $y(t)$ that has finite ε-settling time T_ε also has finite ε-rise time T_r (for the same value of ε) and that $T_r\leqslant T_\varepsilon$. Hence, the ε-rise time is always a lower bound for the ε-settling time.

The goal of this section is to find an upper bound on the ratio of the 1% settling time of the switching architecture to the smallest possible 1% settling time that can be achieved via any bounded control input $|u(t)|\leqslant 1$. In order to establish this bound, we shall find a lower bound on the 1% rise time achievable via bounded control. An upper bound on the ratio will then be the 1% settling time of the switching architecture divided by the lower bound on the 1% rise time for bounded control inputs. As in previous sections, all results will be derived for the case where $a\geqslant b^2$.

4.1.1. Rise time bound. For the plant of Equation (1)

$$P(s)=\frac{a}{s(s-b)}$$

with $a>0$, $b\in\mathbf{R}$, we are interested in deriving a lower bound on the 1% rise time of the step response T_r:

$$T_r=\min_{T\geqslant 0}\{T : y(T)=0.99\}$$

where $y(t)$ is the step response of the plant $P(s)$ when the peak value of the control input $u(t)$ is bounded: $|u(t)|\leqslant 1$ for all $t\geqslant 0$. It is clear that the rise time T_r will be minimized by choosing the input $u(t)$ that maximizes $y(t)$ at each time t subject to the constraint $|u(t)|\leqslant 1$. First, assuming zero initial conditions $y(0)=\dot{y}(0)=0$, note that $y(t)$ can be expressed as the convolution

$$y(t)=\int_0^t \frac{a}{b}(e^{b\tau}-1)u(t-\tau)\,d\tau$$

whenever $b\neq 0$. Now,

$$|y(t)|\leqslant \int_0^t \left|\frac{a}{b}(e^{b\tau}-1)u(t-\tau)\right| d\tau\leqslant \int_0^t \left|\frac{a}{b}(e^{b\tau}-1)\right| d\tau=\int_0^t \frac{a}{b}(e^{b\tau}-1)\,d\tau$$

for any values of $a>0, b\neq 0$. We conclude from the above inequalities that $y(t)$ is maximized for each t by picking $u(t)=1$ for all $t\geqslant 0$. Hence, we can develop a lower bound on the 1% rise time T_r by picking $u(t)=1$ for all $t\geqslant 0$. A similar proof also holds in the case when $b=0$.

Now, when $u(t)=1$ for all $t\geqslant 0$, $y(t)$ can be expressed explicitly as

$$y(t)=\frac{a}{b^2}e^{bt}-\frac{a}{b}t-\frac{a}{b^2}$$

DOI: 10.1002/rnc

For an arbitrary $\varepsilon>0$, the equation we wish to solve to find a bound on the ε-rise time can be expressed as

$$e^{bt}-bt=1+\frac{b^2}{a}(1-\varepsilon) \tag{29}$$

Although a simple closed-form expression for the solution to Equation (29) is not obtainable, using simple inequalities based on the Taylor series expansion of e^x (see [14, Chapter 5] for details), we can arrive at the following lower bound on the ε-rise time T_r:

$$T_r\geqslant\frac{1}{\sqrt{a}}\ln\left(\frac{2+\gamma^2(1-\varepsilon)+\sqrt{(2+\gamma^2(1-\varepsilon))^2-4}}{2}\right) \tag{30}$$

where $\gamma=b/\sqrt{a}$. Note that the constraint $b^2\leqslant a$ is equivalent to the constraint $\gamma\in[-1,1]$.

4.1.2. Upper bound on settling time ratio. If we, again, let $b=\gamma\sqrt{a}$ where $\gamma\in[-1,1]$, then the 1% settling time of the switching architecture T_s of Equation (19) can be reparameterized to be of the form $T_s=h(\gamma)/\sqrt{a}$, where $h(\gamma)$ is given by

$$h(\gamma)=\frac{\gamma+\sqrt{\gamma^2+4}}{2}\left(\ln\left(\frac{100}{\sqrt{2}}\right)+\sqrt{\frac{4+\gamma^2}{4-\gamma^2}}\operatorname{arccot}\left(\frac{2\gamma+\sqrt{\gamma^2+4}}{\sqrt{4-\gamma^2}}\right)\right) \tag{31}$$

Using the above parameterization, we arrive at the following upper bound:

$$\frac{T_s}{T_r}\leqslant\frac{h(\gamma)}{0.95}\triangleq\tilde{h}(\gamma) \tag{32}$$

for all $a>0, \gamma\in[-1,1]$. A plot of $\tilde{h}(\gamma)$ is shown in Figure 13. As the figure shows, $\tilde{h}(\gamma)$ increases with γ. Intuitively, this is sensible since, for fixed a, larger γ corresponds to larger b, and the larger b, the 'more unstable' the plant $P(s)$ of Equation (1). Also, since Figure 13 shows that $\tilde{h}(\gamma)\leqslant10$ for all $\gamma\in[-1,1]$, we can conclude that the 1% settling time of the switching architecture is never more than a factor of 10 larger than the settling time that can be achieved via any control input that is bounded by 1, $|u(t)|\leqslant1$ for all $t\geqslant0$, for any value of $a>0$ and any value of b with $b^2\leqslant a$.

4.2. Time-optimal control, part II: approximate bound on settling time

Although the previous section does provide us with a bound on the ratio of the settling times, as desired, the bound is somewhat conservative. A large part of this is due to the fact that the minimum achievable ε-rise time is, in general, a weak lower bound for the minimum achievable ε-settling time. In this section, we investigate an *approximate* lower bound on the ε-settling time. Although this bound is not exact, this new bound for the ε-settling time can be made arbitrarily close to the true ε-settling time for ε sufficiently small.

For a given plant $P(s)$ of Equation (1), the task of minimizing the ε-settling time of the step response $y(t)$ for some given $\varepsilon\geqslant0$ is the task of finding some control input $u(t)$ with $|u(t)|\leqslant1$ so as to minimize the smallest time T_ε for which $|y(t)-1|\leqslant\varepsilon$ for all $t\geqslant T_\varepsilon$. In general, this is a difficult problem to solve analytically for an arbitrary ε; however, there is one exception for which an analytic solution can be obtained, namely the case when $\varepsilon=0$ exactly. We shall, therefore,

DOI: 10.1002/rnc

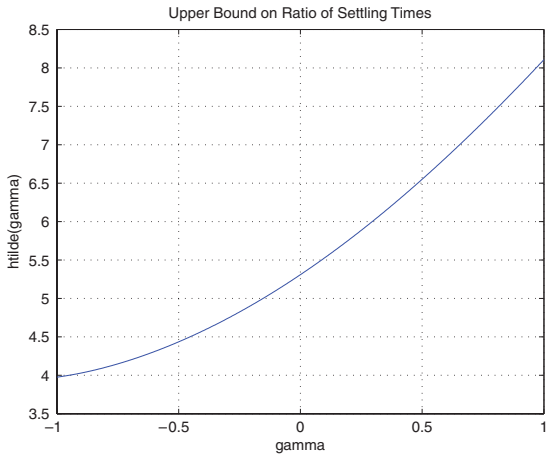

Figure 13. Plot of $\tilde{h}(\gamma)$ of Equation (32) for $\gamma \in [-1, 1]$.

compute the minimal settling time as a function of the plant parameters a and b when $\varepsilon = 0$ and use this as an approximation to the true 1% settling time.

It is true, in theory, that the minimal 1% settling time could be markedly different from the settling time in the case when $\varepsilon = 0$; however, one should naturally expect that when ε is small, the two values should be close. One can show via a continuity argument that when ε is sufficiently small, the minimal ε-settling time of the step response over all control inputs that satisfy $|u(t)| \leqslant 1$ can be made arbitrarily close to the minimal settling time in the case where $\varepsilon = 0$. Moreover, as we shall see when we examine a procedure for designing rational LTI controllers to minimize the settling time in the absence of overshoot, the 1% settling time that can be achieved through the design process is often remarkably close to the bound we derive here.

The formal details of deriving the aforementioned approximate bound are rather lengthy and, hence, are omitted. The interested reader is referred to [14, Chapter 5] for a full derivation. To develop an expression for the approximate bound, recall that T_s, the 1% settling time of the switching architecture, can be parameterized as $h(\gamma)/\sqrt{a}$ where $h(\gamma)$ is given as in Equation (31) where $\gamma = b/\sqrt{a}$. Examine the settling time for the set of a and b such that $a \geqslant b^2$ is equivalent to computing $h(\gamma)$ for $\gamma \in [-1, 1]$.

In a similar fashion, we can derive an approximation T_0 to the ε-settling time T_ε achievable via bounded LTI control, which takes the form $T_0 = f(\gamma)/\sqrt{a}$ where

$$f(\gamma) = \left| \frac{2}{\gamma} \ln \left(\frac{1 + \sqrt{1 - \exp(-\gamma^2)}}{\exp(-\gamma^2/2)} \right) \right|$$

As mentioned above, the ε-settling time can be shown to be continuous at $\varepsilon = 0$, i.e. $T_\varepsilon \approx T_0$ for ε sufficiently small. We therefore approximate the ratio T_s/T_ε via T_s/T_0. For $\gamma \in [-1, 1]$, we have

$$\frac{T_s}{T_0} = \frac{h(\gamma)}{f(\gamma)} \tag{33}$$

A plot of Equation (33) is shown in Figure 14. Comparing this plot with the rise time bound of Figure 13, the approximate bound predicts roughly a factor of two improvements in the ratio of

DOI: 10.1002/rnc

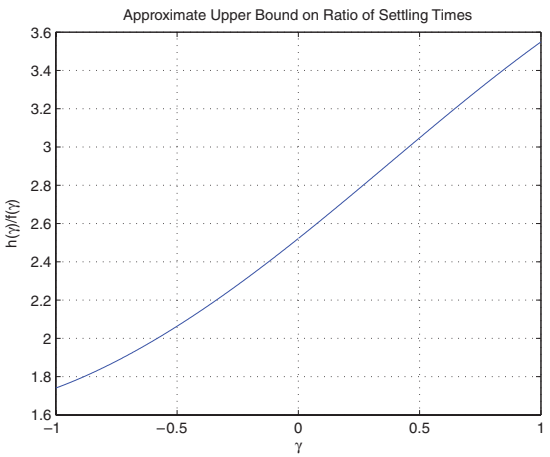

Figure 14. Plot of $h(\gamma)/f(\gamma)$ for $\gamma \in [-1, 1]$.

the 1% settling time of the switching architecture to the achievable 1% settling time of arbitrary bounded control with $|u(t)| \leqslant 1$. For instance, although the weak bound predicts a factor of 8 difference for the case when $\gamma = 1$, the approximate bound predicts roughly a factor of 3.5 when $\gamma = 1$, down from roughly one order of magnitude difference to roughly half an order of magnitude. Although again, it must be advised that the approximate bound may actually differ from the true ratio quite significantly, we shall see in the following section that the bound shown in Figure 14 is often very close to the true ratio.

4.3. Designing LTI controllers with minimum settling time

We now turn to the problem of *designing* LTI controllers that minimize the 1% settling time of the step response for a given plant $P(s)$ of the form of Equation (1). Formally, the problem we wish to investigate is this: for a given plant $P(s)$, we wish to design an LTI controller $K(s)$ connected in the servo configuration of Figure 5 such that when the input $r(t)$ is a unit step and the plant and controller are both initially at rest, the following constraints are satisfied:

1. The closed-loop transfer function $S(s)$ from $r(t)$ to $y(t)$ is stable.
2. The control signal $u(t)$ is bounded: $|u(t)| \leqslant 1$ for all $t \geqslant 0$.
3. The 1% settling time is made as small as possible, i.e. the value of T for which $|y(t) - 1| \leqslant 0.01$ for all $t \geqslant T$ is minimized.
4. The percentage overshoot is less than 1%, i.e. $y(t) \leqslant 1.01$ for all $t \geqslant 0$.

For a given value of T, note that items 2–4 are linear constraints on the step response of the control input $u(t)$ and plant output $y(t)$. As we shall see now, the problem we solve here can be represented as an infinite-dimensional linear programming problem which, upon appropriate discretization, yields an algorithm that can be implemented in MATLAB for finding $K(s)$ which satisfies all the above constraints. All the techniques we discuss here are presented in more detail in [24].

DOI: 10.1002/rnc

4.3.1. Characterization of stabilizing controllers. First, we shall recall the classical *interpolation conditions* that state the following: for the feedback interconnection of Figure 5, consider the closed-loop transfer function $S(s)$ given by

$$S(s)=\frac{P(s)K(s)}{1+P(s)K(s)}$$

where $K(s)$ is a proper stabilizing controller and $P(s)$ has relative degree r. If we denote by $p_1, p_2, \ldots, p_n$ and $z_1, z_2, \ldots, z_m$ the unstable poles and zeros of the plant $P(s)$, respectively (i.e. those poles and zeros that lie in the closed right half-plane), then the following conditions must be satisfied:

1. $S(s)$ is stable.
2. $S(p_1)=S(p_2)=\cdots=S(p_n)=1$.
3. $S(z_1)=S(z_2)=\cdots=S(z_m)=0$.
4. The relative degree of $S(s)$ is at least r.

Using these conditions, we may express any stable closed-loop transfer function $S(s)$ in terms of the so-called *Q-parameterization* [25]:

$$S(s)=\sum_{i=r}^{\infty} a_i Q_i(s) \tag{34}$$

where $\{Q_i(s)\}_{i=1}^{\infty}$ forms a complete basis for the set of stable transfer functions RH^{∞} and where Equation (34) satisfies the interpolation constraints above. One such basis, known as the *Ritz basis* [24], is given by

$$Q_i(s)=\left(\frac{c}{s+c}\right)^i \tag{35}$$

for any $c\in\mathbf{R}$, $c\neq 0$. We shall use this basis for performing the numerical computations to be described.

4.3.2. Formulation of linear programming problem. We utilize the results of the previous section in the following way. For some integer $N>0$ that is potentially large, we consider the set of closed-loop transfer functions $S(s)$ from $r(t)$ to $y(t)$ in Figure 5 of the form

$$S(s)=\sum_{i=2}^{N} a_i Q_i(s)$$

where a_i are the coefficients to be determined. For the plant $P(s)$ of Equation (1), we have the interpolation condition

$$\sum_{i=2}^{N} a_i Q_i(0)=\sum_{i=2}^{N} a_i=1$$

When $b>0$, we have the additional interpolation condition

$$\sum_{i=2}^{N} a_i Q_i(b)=\sum_{i=2}^{N} a_i\left(\frac{c}{c+b}\right)^i=1$$

DOI: 10.1002/rnc

To represent the conditions imposed on the step response $y(t)$ and the control signal $u(t)$, let $s_i(t)$ represent the step response of $Q_i(s)$ and $u_i(t)$ represent the step response of $Q_i(s)/P(s)$. For a given settling time T, we can represent the control bound, the 1% settling time, and the overshoot constraint as

$$\left|\sum_{i=2}^{N} a_i u_i(t)\right| \leqslant 1 \quad \forall t \geqslant 0$$

$$\left|1-\sum_{i=2}^{N} a_i s_i(t)\right| \leqslant 0.01 \quad \forall t \geqslant T$$

$$\sum_{i=2}^{N} a_i s_i(t) \leqslant 1.01 \quad \forall t \geqslant 0$$

respectively. All the above constraints are linear constraints on the coefficients a_i and, hence, form an infinite-dimensional linear program. By finely gridding the time axis, one may approximate this by a finite-dimensional linear program, which can be solved via existing software packages such as MATLAB's `sedumi` package. If the problem is feasible, the coefficients a_i determine for us a closed-loop transfer function whose output step response $y(t)$ and control step response $u(t)$ satisfy the desired conditions for some settling time T. A stabilizing controller $K(s)$ may then be obtained using

$$K(s) = \frac{S(s)}{P(s)(1-S(s))}$$

4.3.3. Results. We present the results of using the above algorithm for five different plants in Table I. The table shows four quantities for each plant: the approximate settling time T_0 described in the last section, the minimum 1% settling time that was achieved using the linear programming formulation, the smallest order of a controller that could be found, which achieves the minimal settling time, and the 1% settling time of the switching architecture we derived at the beginning of the section (for reference). Note that the minimum 1% settling times are not too far from the approximate bound T_0; the largest deviation of the five plants is about 7.5%, and the approximate bound on the ratio of the settling times that we derived earlier is off by less than 10%.

Table I. Summary of results for five different plants $P(s)$.

$P(s)$	Approximation T_0	Measured 1% settling time	Controller order	Switching architecture 1% settling time T_s
$\frac{1}{s^2}$	2	1.85	17	5.08
$\frac{100}{s(s+1)}$	0.2002	0.185	17	0.4849
$\frac{1}{s(s+1)}$	2.1701	2.04	15	3.7772
$\frac{100}{s(s-1)}$	0.2002	0.193	22	0.5253
$\frac{1}{s(s-1)}$	2.1701	2.08	38	7.7013

The approximation T_0 refers to the approximate 1% settling time described in Section 4.2.

DOI: 10.1002/rnc

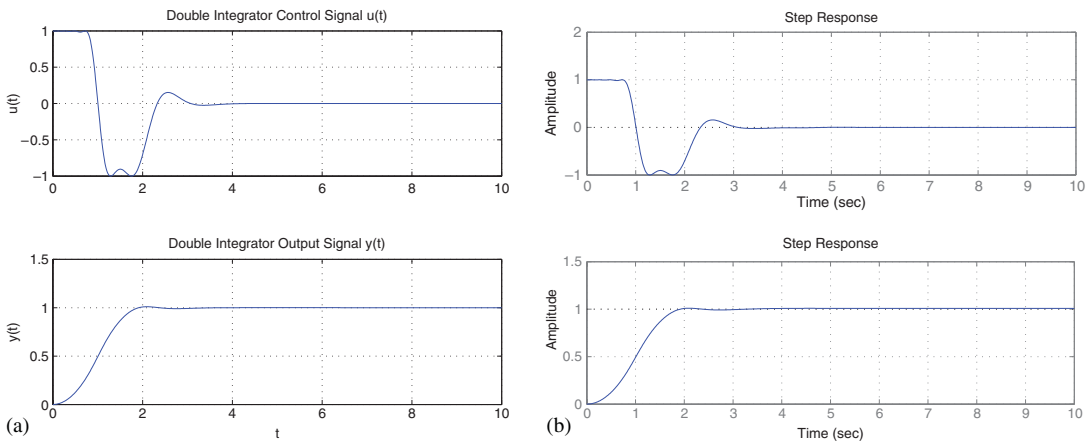

Figure 15. (a) Control signal $u(t)$ and step response $y(t)$ which yield minimal 1% settling time (1.85 s) for the double integrator $P(s)=1/s^2$ using a 17th-order controller and (b) control signal $u(t)$ and step response $y(t)$ which yield minimal 1% settling time (1.85 s) for the double integrator $P(s)=1/s^2$ using a reduced-order controller (12th order).

After the 1% settling time was determined for each plant, the minimal controller order was determined by reducing the value of N until the program became infeasible. The controller order for the smallest value of N, which did not make the program become infeasible, is what is listed in the table. Extrapolating from the examples shown here, we see that the order of the controller needed to achieve the minimal 1% settling time using this method is, generally, quite high. Using standard model reduction techniques on the controller can provide some reduction in the order of the optimal controller. For instance, using Hankel model order reduction techniques, one can reduce the optimal controller for the double integrator down from a 17th-order controller to a 12th-order controller. The control step response $u(t)$ and the output step response $y(t)$ are shown for the 17th-order controller in Figure 15(a) and for the 12th-order controller in Figure 15(b). Similar reductions in order were observed when performing Hankel model order reduction on the optimal controllers for the other plants.

A natural question to ask at this point is as follows: how does the controller order change with the settling time? Can we increase the settling time and dramatically decrease the order of the optimal controller using this method? The answer to this question is, in general, no. By increasing the settling time, it is possible to decrease the order of the required controller, but the order of the resulting controller is still generally fairly high using the method shown here. For instance, in the case of the double integrator, by increasing the 1% settling time to 2.53 s, we were able to design a 10th-order controller (which could be reduced to a ninth-order controller via Hankel model reduction), but an attempt to increase the settling time beyond that point did not reduce the order of the optimal controller at all.

5. CONCLUSION AND FUTURE WORK

To briefly summarize the findings we have presented here, we studied a control design problem for three different classes of controllers in which we compared the performance of a particular

DOI: 10.1002/rnc

switching architecture with the performance that can be achieved via two other forms of LTI control. We showed that, for a class of plants, the first-order switching architecture we presented here outperforms what can be achieved by first-order LTI control, hence showing that the addition of switching can provide performance benefits. We also showed that while, in general, bounded LTI control of unconstrained order can outperform the first-order switching architecture, the performance increase is bounded. Moreover, we investigated a method of designing close-to-optimal controllers which, as we showed through the context of several examples, yields controllers of rather high order.

One question that the interested reader may be wondering about in regard to the switching system of Section 2 is whether it suffers from the phenomenon of *chatter* when time delays are present. Such behavior is typically observed in sliding mode control systems when the control law creates a vector field, which geometrically points at the stable manifold from either side of the manifold (see [26] for a discussion and illustrations of chatter). It can be shown for the switching law of Equation (6), however, that the composite vector field composed of $(A+v_0BC)z$ in the region $z'(\tilde{w}_s\tilde{q}')z\leqslant 0$ and $(A-v_0BC)z$ in the region $z'(\tilde{w}_s\tilde{q}')z>0$ always points in either a clockwise orientation or a counterclockwise orientation throughout the entire state space. Hence, one may expect that the control law equation (6) will not be chatter sensitive. Although a formal comparison/proof of this statement has not yet been constructed, several numerical simulations indicate strongly that Equation (6) is very insensitive to chatter. This result is a great contrast to many existing results on the design of switched static gain controllers for second-order linear systems (see, e.g. [16, 17] and the figures therein) in which chatter is a *fundamental* characteristic of the control law rather than simply an artifact of time delays. A formal study of this switching architecture's sensitivity to chatter is an important area of future research.

Also, to briefly return to the issue of non-uniqueness of the vector $\tilde{q}$ in Equation (6), note that although the exact choice of $\tilde{q}$ (and, hence, q) does not affect the 1% settling time or overshoot of the corresponding step response, the choice of q *does* affect the value of the $L2$ gain computed in Section 3. Numerical simulation currently indicates that, if one takes the vector q to lie very close in angle to either w_s or w_u, the $L2$ gain becomes very large. Hence, one could attempt to find q which minimizes the $L2$ gain calculation of Section 3 to increase the performance gap between the switching architecture and the achievable performance of first-order servo control. The choice of q used in this exposition was not optimized (it was based on a simple angle bisector heuristic; see [14, Chapter 3]), but it is clear that characterizing the $L2$ gain as a function of the parameter q has important ramifications.

It should be noted that, although the work we present here was derived for a simple class of second-order LTI plants, it is possible to extend the results shown here to a broader class of systems. Indeed, using the $L2$ gain tools for the class of switching controllers shown here as developed in [14, Chapter 4], one can apply the standard tools of perturbation theory via the Small Gain Theorem to extend to a class of systems that are well approximated by a second-order LTI model. Chapter 6 of [14] presents an example in which a switching architecture of the form shown here is used to robustly stabilize a class of fourth-order LTI plants. Complete formal studies/comparisons for wider sets of plants is a task that is yet to be completed and is a direction that should be taken.

Although the comparison here demonstrates promise for the switching architecture that we show here in the context of both a particular plant set and a particular performance objective, the general utility of this structure and/or similar architectures for a wider range of performance problems is still very much an open area of research. Much of the work developed here was inspired by applications for the electronics industry, and, as such, one of the future goals is to examine other

DOI: 10.1002/rnc

application areas that have the potential to benefit from switching structures similar to the one we showed here.

APPENDIX A

A.1. Proof of Proposition 3.1

To prove item 1, we shall prove the following equivalent fact: that the peak control value occurs at time 0, i.e. $|u(t)|<k$ for all $t>0$ (note the strict inequality). To begin, note again that the transfer function from $r(t)$ to $u(t)$ in Figure 6 is given by

$$H_{ru}(s)=\frac{ks^2(s+c)}{s^3+ds^2+ks+kc}$$

In order for the above transfer function to represent an asymptotically stable system, we can deduce from the Routh criterion that $c>0, d>0, k>0$, and $d>c$. The zero-state unit step response of the above transfer function can be characterized via the dynamics of the autonomous system

$$\begin{aligned}\dot{z}_1&=(c-d)z_1-z_2-c(c-d)z_3\\ \dot{z}_2&=kz_1\\ \dot{z}_3&=z_1-cz_3\\ u&=kz_1\end{aligned}$$

with initial condition $z_1(0)=1$, $z_2(0)=z_3(0)=0$.

We shall use the above state-space description in z coordinates to argue that $|u(t)|<k$ for all $t>0$. Assume that the constraint does *not* hold, i.e. that there exists some time $t_0>0$ for which $u(t_0)=k$ or $u(t_0)=-k$. Suppose for the moment that $z_2(t_0)=z_3(t_0)=0$. Then the state of the system $z=[z_1\ \ z_2\ \ z_3]'$ would satisfy the relationship $z(t_0)=\pm z(0)$. Moreover, the time invariance of this system would imply that $z(mt_0)=\pm z(0)\neq 0$ for all $m\in\mathbf{Z}^+$, which would contradict the assumed asymptotic stability of the original system.

As it turns out, if $u(t_0)=\pm k$, then the remaining states $z_2(t_0)$ and $z_3(t_0)$ *must* be 0, as we now show. Consider the quadratic Lyapunov function

$$V(z)=z_1^2+\frac{1}{k}z_2^2+c(d-c)z_3^2$$

which, along the system trajectories, satisfies

$$\dot{V}(z)=2(c-d)(z_1-cz_3)^2\leqslant 0$$

for all $z\in\mathbf{R}^3$. Note that $V(z)$ satisfies the property that

$$V(z_1,z_2,z_3)>V(z_1,0,0)\quad\forall(z_2,z_3)\in\mathbf{R}^2\backslash\{0\}$$

Now, suppose that $u(t_0)=k$ or, correspondingly, that $z_1(t_0)=1$, and that either or both of $z_2(t_0)$ and $z_3(t_0)$ are non-zero. Then we have that

$$V(1,z_2(t_0),z_3(t_0))>V(1,0,0)$$

DOI: 10.1002/rnc

which contradicts the fact that $V(z)$ is non-increasing along the system trajectories. By noting that $V(z)=V(-z)$, a similar proof holds to show that if $u(t_0)=-k$ then a similar contradiction holds. Hence, it follows that if $u(t_0)=\pm k$, then $z_2(t_0)=z_3(t_0)=0$, and we conclude that $u(t_0)$ cannot equal either k or $-k$ for any $t_0>0$. By the continuity of the state trajectories, we further conclude that $|u(t)|<k$ for all $t>0$ and that the peak control value (which occurs at time 0) is equal to k.

To prove the second item, let $H_1(s)=P(s)/(1+P(s)K(s))$ and define $G_1(s)=H_1(\sqrt{k}s)$. It is clear that $\|G_1(s)\|_\infty=\|H_1(s)\|_\infty$. Note that $G_1(s)$ can be expressed in the form

$$G_1(s)=\frac{s+d/\sqrt{k}}{s^3+(d/\sqrt{k})s^2+s+c/\sqrt{k}}=\frac{P(s)}{1+P(s)\tilde{K}(s)}$$

from which the norm-bound constraint in item 2 immediately follows. Note also that $\tilde{K}(s)$ is a special form of Equation (20) with $k=1$; hence, by the result of item 1, the peak control value is equal to 1. Hence, $\tilde{K}(s)$ satisfies both constraints that we are imposing on the closed-loop system of Figure 6.

Now, if we define the transfer functions

$$H_2(s)=\frac{P(s)K(s)}{1+P(s)K(s)},\quad G_2(s)=\frac{P(s)\tilde{K}(s)}{1+P(s)\tilde{K}(s)}$$

which represent the closed-loop transfer functions from $r(t)$ to $y(t)$ in Figure 6 for the controllers $K(s)$ and $\tilde{K}(s)$, respectively, then a simple calculation shows that $G_2(s)=H_2(\sqrt{k}s)$. Let $s(t)$ be the unit step response of the system with transfer function $H(s)$ and $\tilde{s}(t)$ be the unit step response of the system with transfer function $G(s)$, i.e.

$$s(t)=\int_0^t h_2(\tau)\,\mathrm{d}\tau,\quad \tilde{s}(t)=\int_0^t g_2(\tau)\,\mathrm{d}\tau$$

where $h_2(t)$ and $g_2(t)$ are the impulse responses corresponding to the transfer functions $H_2(s)$ and $G_2(s)$, respectively. Because the impulse responses satisfy the relationship

$$g_2(t)=\frac{1}{\sqrt{k}}h_2\left(\frac{t}{\sqrt{k}}\right)$$

we have

$$\tilde{s}(t)=\int_0^t g_2(\tau)\,\mathrm{d}\tau=\int_0^t \frac{1}{\sqrt{k}}h_2\left(\frac{\tau}{\sqrt{k}}\right)\mathrm{d}\tau=\int_0^{t/\sqrt{k}} h_2(\sigma)\,\mathrm{d}\sigma=s\left(\frac{t}{\sqrt{k}}\right)$$

The above relationship makes clear that if the step response $s(t)$ has percentage overshoot M and 1% settling time T, then the step response $\tilde{s}(t)$ also has percentage overshoot M and 1% settling time $T\sqrt{k}$.

ACKNOWLEDGEMENTS

The authors would like to thank Profs. Alexandre Megretski and George Verghese for the many useful comments that they made during the period leading up to and including this work. The authors would also like to thank the anonymous reviewers for their many useful comments in helping to improve the quality of this paper.

DOI: 10.1002/rnc

REFERENCES

1. Branicky MS. Multiple Lyapunov functions and other tools for switched and hybrid systems. *IEEE Transactions on Automatic Control* 1998; **43**(4):475–482.
2. Chatterjee D, Liberzon D. Stability analysis of deterministic and stochastic switched systems via a comparison principle and multiple Lyapunov functions. *SIAM Journal on Control and Optimization* 2006; **45**(1):174–206.
3. Goncalves JM, Megretski A, Dahleh MA. Global stability of relay feedback systems. *IEEE Transactions on Automatic Control* 2001; **46**(4):550–562.
4. Goncalves JM, Megretski A, Dahleh MA. Global analysis of piecewise linear systems using impact maps and surface Lyapunov functions. *IEEE Transactions on Automatic Control* 2003; **48**(12):2089–2106.
5. Hespanha JP. Logic-based switching algorithms in control. *Ph.D. Dissertation*, Yale University, 1998.
6. Hespanha JP, Morse AS. Switching between stabilizing controllers. *Automatica* 2002; **38**(11):1905–1917.
7. Artstein Z. Example of stabilization with hybrid feedback. *Hybrid Systems III*: *Verification and Control*, Lecture Notes in Computer Science, vol. 1066. Springer: Berlin, 1996; 173–185.
8. Hu B, Zhai G, Michel AN. Hybrid output feedback stabilization of two-dimensional linear control systems. *Proceedings of the 2000 American Control Conference*, Chicago, 2000; 2184–2188.
9. Hu B, Zhai G, Michel AN. Hybrid output feedback stabilization of second-order linear time-invariant systems. *Linear Algebra and its Applications* 2002; **351–352**:475–485.
10. Liberzon D. Stabilizing a linear system with finite-state hybrid output feedback. *Proceedings of the 7th IEEE Mediterranean Conference on Control and Automation*, Haifa, Israel, 1999.
11. Litsyn E, Nepomnyashchikh YV, Posonov A. Stabilization of linear differential systems via hybrid feedback controls. *SIAM Journal on Control and Optimization* 2000; **38**(5):1468–1480.
12. Santarelli KR, Megretski A, Dahleh MA. On the stabilizability of two-dimensional linear systems via switched output feedback. *Proceedings of the 24th American Control Conference*, vol. 6, Portland, OR, 2005; 3778–3783.
13. Santarelli KR, Dahleh MA, Megretski A. Optimal controller synthesis for second order LTI plants with switched output feedback. *Proceedings of the 46th Conference on Decision and Control*, San Diego, 2007; 4127–4132.
14. Santarelli KR. On the synthesis of switched output feedback controllers for linear, time-invariant systems. *Ph.D. Thesis*, Massachusetts Institute of Technology, 2007.
15. Xu X, Antsaklis PJ. Design of stabilizing control laws for second-order switched systems. *Proceedings of the 14th IFAC World Congress*, vol. C, Beijing, 1999; 181–186.
16. Xu X, Antsaklis PJ. Stabilization of second-order LTI switched systems. *ISIS Technical Report isis-99-001*. Department of Electrical Engineering, University of Notre Dame, 1999.
17. Zhai G, Kondo H, Imae J, Kobayashi T. Hybrid static output feedback stabilization of two-dimensional LTI systems: a geometric method. *International Journal of Control* 2006; **79**(8):982–990.
18. Benassi C, Gavioli A. Hybrid stabilization of planar linear systems with one-dimensional outputs. *Systems and Control Letters* 2002; **46**:303–309.
19. Litsyn E, Nepomnyashchikh YV, Posonov A. Classification of linear dynamical systems in the plane admitting a stabilizing hybrid feedback control. *Journal of Dynamical Systems* 2000; **6**(4):477–501.
20. Santarelli K, Dahleh MA. Comparison between a switching controller and two LTI controllers for a class of LTI plants. *Proceedings of the 2008 American Control Conference*, Seattle, WA, June 2008.
21. Gray PR, Meyer RG. *Analysis and Design of Analog Integrated Circuits* (3rd edn). Wiley: New York, 1993.
22. Johns DA, Martin K. *Analog Integrated Circuit Design*. Wiley: New York, 1997.
23. Siebert W. *Circuits*, *Signals and Systems*. The MIT Press: Cambridge, MA, 1986.
24. Boyd S, Barrat C. *Linear Controller Design*: *Limits of Performance*. Prentice-Hall: Englewood Cliffs, NJ, 1991.
25. Zhou K, Doyle C. *Essentials of Robust Control*. Prentice-Hall: Englewood Cliffs, NJ, 1998.
26. Khalil HK. *Nonlinear Systems* (2nd edn). Prentice-Hall: Englewood Cliffs, NJ, 1996.

DOI: 10.1002/rnc